Gouy phase in nonclassical paths in a triple-slit interference experiment

I. G. da Paz,[1] C. H. S. Vieira,[1] R. Ducharme,[2] L. A. Cabral,[3] H. Alexander,[4] and M. D. R. Sampaio[4]

[1]*Departamento de Física, Universidade Federal do Piauí, Campus Ministro Petrônio Portela, CEP 64049-550, Teresina, Piauí, Brazil*

[2]*2112 Oakmeadow Place, Bedford, Texas 76021, USA*

[3]*Curso de Física, Universidade Federal do Tocantins, Caixa Postal 132, CEP 77804-970, Araguaína, Tocantins, Brazil*

[4]*Departamento de Física, Instituto de Ciências Exatas, Universidade Federal de Minas Gerais, Caixa Postal 702, CEP 30161-970, Belo Horizonte, Minas Gerais, Brazil*

(Received 14 October 2015; published 14 March 2016)

We propose a simple model to study the Gouy phase effect in the triple-slit experiment in which we consider a nonclassical path. The Gouy phase differs for classical and nonclassical paths as it depends on the propagation time. In this case the Gouy phase difference changes the Sorkin parameter κ used to estimate the nonclassical path contribution in a nontrivial way, shedding some light on the implementation of experiments to detect nonclassical path contributions.

DOI: 10.1103/PhysRevA.93.033621

I. INTRODUCTION

The Gouy phase shift in light optics was theoretically studied and experimentally observed by Gouy in 1890 [1,2]. The physical origin of this phase was studied in [3–10]. The Gouy phase shift appears in any kind of wave that is submitted to transverse spatial confinement, either by focusing or by diffraction through small apertures. When a wave is focused [5], the Gouy phase shift is associated with the propagation from $-\infty$ to $+\infty$ and is equal to $\pi/2$ for cylindrical waves (line focus) and π for spherical waves (point focus). In the case of diffraction by a slit it was shown that the Gouy phase shift is $\pi/4$, and it is dependent on the slit width and the propagation times before and after the slit [11]. The Gouy phase shift has been observed in different kinds of waves such as water waves [12]; acoustic [13], surface plasmon-polariton [14], and phonon-polariton [15] pulses; and, recently, matter waves [16–18].

Applications of the Gouy phase in light optics opening the possibility of development of optical systems has been the subject of many studies and increasing interest. For instance, the Gouy phase has to be taken into account to determine the resonant frequencies in laser cavities [19] or the phase matching in high-order-harmonic generation (HHG) [20] and to describe the spatial variation of the carrier-envelope phase of ultrashort pulses in a laser focus [21]. Moreover, the Gouy phase plays an important role in the evolution of optical vortex beams [22] as well as electron beams which acquire an additional Gouy phase dependent on the absolute value of the orbital angular momentum [17]. Gravity-wave-detection antennas are based on precision measurements using laser interferometry in which the Gouy phase is crucial [23].

In the nonrelativistic matter-wave context the Gouy phase was explored first in [24,25], followed by experimental realizations with Bose-Einstein condensates [16], electron vortex beams [17], and astigmatic electron matter waves using in-line holography [18]. Recently, it was shown that the Beteman-Hillion solutions to the Klein-Gordon equation present a Gouy phase that includes relativistic effects [26]. Matter-wave Gouy phases have interesting applications as well. For instance, they serve as mode conversers important in quantum information [25], in the development of singular electron optics [18], and in studying the Zitterbewegung phenomenon [26], and now we investigate how important it can be in the study of nonclassical paths in interference experiments such as less likely, more exotic looping paths, as we shall explain below. From the theoretical viewpoint, the contribution of such exotic trajectories amounts to saying that the superposition principle is usually incorrectly applied in interference experiments.

A theoretical treatment of the nonclassical path in the double slit was studied in [27]. The authors estimated a nonlinear interference term to test a deviation from the superposition principle in the double-slit experiment. They used the Feynman path-integral approach [28] with inclusion of paths looping along the slits, i.e., nonclassical paths. Experimental access to such tiny deviations was discussed by Sorkin [29] in a work where higher-order phenomena incorporate the usual prescription of interference when three or more paths interfere. However, only recently was a quantification of the nonclassical paths in interference experiments for a triple slit proposed [30–33].

The theoretical analysis to support these experiments is based on path integrals in the presence of slits with different weights for classical and nonclassical paths; namely, the propagator is written as

$$K(\vec{r}_1,\vec{r}_2) = \int \mathcal{D}[\vec{x}(s)] \exp\left[ik \int ds\right],$$

where s is the contour length along $\vec{x}(s)$, with the classical limit being $k \to \infty$, where paths near the straight line linking $\vec{r}_1$ to $\vec{r}_2$ contribute via the stationary phase. Paths away from the classical path contribute a rapidly oscillating phase. All paths from source to detector should be considered, excluding those that would cross the opaque walls along the slits.

Reference [30] introduced the Sorkin factor κ, which gauges the deviation of the Born rule for probabilities in quantum mechanics, i.e., to estimate contributions from nonclassical paths. $\kappa = 0$ if only classical paths contribute to the final interference pattern in the detector, and $\kappa \neq 0$ if, beyond the usual classical paths, nonclassical paths are considered in the calculations and contribute to the final result. Although the effect of nonclassical paths can also appear

for the usual double-slit experiment, until the present time no deviation from a null value of κ was detected in this setup. However, new experiments with three slits proposed in [33] using matter waves or low-frequency photons were analytically described, enabling us to set an upper bound on the Sorkin factor $|\kappa_{max}| \approx 0.003\lambda^{3/2}/(d^{1/2}w)$, in which λ is the wavelength, d is the center-to-center distance between the slits, and w is the width of the slit. Those experiments confirmed that κ is very sensitive to the experimental setup.

Triple-slit (path) experiments have become a useful testing ground for checking Born's rule in quantum mechanics [29,30,34,35]. In Ref. [32] the nonclassical contributions for triple-slit matter-wave diffraction were evaluated using the Feynman path-integral approach with a free propagator given by $K(\vec{r},\vec{r}') = \frac{k}{2\pi i}\frac{1}{|\vec{r}-\vec{r}'|}e^{ik|\vec{r}-\vec{r}'|}$ (which satisfies the Helmholtz equation away from $\vec{r} = \vec{r}'$ and the Fresnel-Huygens principle). In the Fraunhofer regime this leads to integrals which are evaluated numerically using stationary phase approximation. As a result they obtain $\kappa \approx 10^{-8}$ for electron waves [32].

The guiding purpose of this paper is to incorporate the effect of the Gouy phase into parameter κ and indicate this effect on the pattern of interference as well in κ for matter waves. As we shall see, the Sorkin factor for triple-slit interference is dependent on the Gouy phase difference between classical and nonclassical paths. The effect of the Gouy phase of matter waves has recently earned prominence with its inclusion in electron beams, which are used in [32,33] to estimate $\kappa \approx 10^{-8}$. In order to analytically evaluate the interference pattern we establish a procedure similar to that presented in [11,36] using nonrelativistic propagators for a free-particle Gaussian wave packet adapted to triple-slit interference with nonclassical paths. This framework allows for exact integration and analytical expressions which depend on the geometry of the experimental setup and source parameters. Moreover, we make explicit the Gouy phase in the wave functions for a triple-slit apparatus ψ_1, ψ_2, ψ_3, and ψ_{nc} (the corresponding wave function for nonclassical path) and derive an expression for κ which is of the order of 10^{-8} for electron waves. Our nonrelativistic propagator, which satisfies the Schrödinger equation accurately, describes matter-wave interferometry in this experimental regime [37,38], and Gaussian apertures allow for direct analytical integration. Moreover, the Gouy phase has a simple analytical expression. Therefore we have used the three-slit experimental setup in order to compare the order of magnitude of our κ parameter with the one obtained in [32] for the same input data and verified that they agree for electron waves.

This contribution is organized as follows: in Sec. II we obtain analytical expressions for the wave functions for classical and nonclassical paths and calculate the intensity. We estimate the deviations produced by nonclassical path through the Sorkin parameter κ. In Sec. III we analyze the effect of the Gouy phase on the Sorkin parameter for electron waves, and we estimate the percentage error in this parameter when we neglect the Gouy phase difference of classical and nonclassical paths in order to get some insight into the relative importance of such effects in the interference pattern. We draw some concluding remarks in Sec. IV.

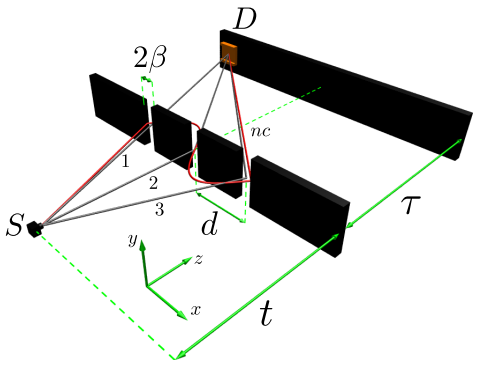

FIG. 1. Sketch of triple-slit experiment. Gaussian wave packet of transverse width σ_0 produced in the source S propagates a time t before attaining the triple slit and a time τ from the triple slit to the detector D. The slit apertures are taken to be Gaussian of width β separated by a distance d. Paths 1, 2, and 3 are classical paths, and the path 123 is one of the several possible nonclassical paths.

II. NONCLASSICAL PATHS IN THE TRIPLE-SLIT EXPERIMENT

In this section we obtain analytical results for the wave functions of classical and nonclassical paths in the triple-slit experiment while keeping track of phases in order to assess their role in the interference pattern. For the purpose of this paper we suppose a one-dimensional model in which quantum effects are manifested only in the x direction, as depicted in Fig. 1. A coherent Gaussian wave packet of initial transverse width σ_0 is produced in the source S and propagates during a time t before arriving at a triple slit with Gaussian apertures from which Gaussian wave packets propagate. After crossing the grid the wave packets propagate during a time τ before arriving at detector D in the detection screen, giving rise to an interference pattern as a function of the transverse coordinate x. Quantum effects are realized only in the x direction as we consider that the energy associated with the momentum of the particles in the z direction is very high, such that the momentum component p_z is sharply defined, i.e., $\Delta p_z \ll p_z$. Then we can consider a classical movement in this direction at velocity v_z. Because the propagation is free, the x, y, and z dimensions decouple for a given longitudinal location, and thus, we may write $z = v_z t$. As v_z is assumed to be a well-defined velocity, we can neglect statistical fluctuations in the time of flight, i.e., $\Delta t \ll t$. Such an approximation leaves the Schrödinger equation analogous to the optical paraxial Helmholtz equation [38,39]. For a more general treatment one can follow the model studied in Ref. [40]. The summation over all possible trajectories allows for exotic paths such as the one depicted in Fig. 1. Although there are several possibilities of nonclassical paths for the triple slits, we focus on the windy path 123 in Fig. 1. We calculate the corresponding wave function for this path in order to analyze its effect in the interference pattern.

The wave functions corresponding to classical paths (gray lines) 1 and 3 read ($\int_{-\infty}^{+\infty}\cdots\int_{-\infty}^{+\infty} dx_1\cdots dx_n \equiv \int_{x_1\ldots x_n}$)

$$\psi_{1,3}(x,t,\tau) = \int_{x_j,x_0} K_\tau(x,t+\tau;x_j,t)F(x_j \pm d) \times K_t(x_j,t;x_0,0)\psi_0(x_0), \quad (1)$$

whereas for classical path 2

$$\psi_2(x,t,\tau) = \int_{x_j,x_0} K_\tau(x,t+\tau;x_j,t)F(x_j) \times K_t(x_j,t;x_0,0)\psi_0(x_0), \quad (2)$$

with

$$K(x_j,t_j;x_0,t_0) = \sqrt{\frac{m}{2\pi i\hbar(t_j-t_0)}}\exp\left[\frac{im(x_j-x_0)^2}{2\hbar(t_j-t_0)}\right], \quad (3)$$

$$F(x_j) = \exp\left[-\frac{(x_j)^2}{2\beta^2}\right], \quad (4)$$

and

$$\psi_0(x_0) = \frac{1}{\sqrt{\sigma_0\sqrt{\pi}}}\exp\left(-\frac{x_0^2}{2\sigma_0^2}\right). \quad (5)$$

The kernels $K_t(x_j,t;x_0,0)$ and $K_\tau(x,t+\tau;x_j,t)$ are the free propagators for the particle, and the functions $F(x_j)$ describe the slit transmission functions, which are taken to be Gaussian of width β separated by a distance d; σ_0 is the effective width of the wave packet emitted from the source S, m is the mass of the particle, and t (τ) is the time of flight from the source (triple slit) to the triple slit (screen). The wave function associated with nonclassical path 123 (red line) is given by

$$\psi_{nc}(x,t,\tau) = \int_{x_0,x_1,x_2,x_3} K_\tau(x,\tau+\tilde{t};x_3,\tilde{t}) \times F(x_3+d)F(x_2)K(1\to 2;2\to 3) \times F(x_1-d)K_t(x_1,t+\eta;x_0,0)\psi_0(x_0), \quad (6)$$

where $\tilde{t} = t + 2(\epsilon+\eta)$ and

$$K(1\to 2;2\to 3) = \sqrt{\frac{m}{4\pi i\hbar(\epsilon+\eta)}} \times \exp\left[\frac{im[(x_2-x_1)^2+(x_3-x_2)^2]}{4\hbar(\epsilon+\eta)}\right] \quad (7)$$

is the free propagator which propagates from slit 1 to slit 2 and from slit 2 to slit 3. The parameter $\eta\to 0$ is an auxiliary interslit time parameter, and ϵ is the time spent from one to the next slit and is determined by the momentum uncertainty in the x direction, i.e., $\epsilon = \frac{d}{\Delta v_x}$ ($\Delta v_x = \Delta p_x/m$), where $\Delta p_x = \sqrt{\langle\hat{p}_x^2\rangle - \langle\hat{p}_x\rangle^2}$, with $\hat{p}_x$ being the momentum operator in the x direction. The time ϵ is a statistical fluctuation of the time for the movement in the x direction which has to attain a minimum value $d/\Delta v_x$ in order to guarantee the existence of a nonclassical path. This estimation is compatible with the propagation which builds the nonclassical trajectory. A similar argument was used in [41], where nonclassical dynamics based on the uncertainty principle are considered in an interferometer. Trajectories winding around the slits evidently contribute less and less to the interference pattern.

After some lengthy algebraic manipulations, we obtain

$$\psi_1(x,t,\tau) = A\exp(-C_1x^2 - C_2x + C_3) \times \exp(i\alpha x^2 - i\gamma x - i\theta_c + i\mu_c), \quad (8)$$

$$\psi_2(x,t,\tau) = A\exp(-C_1x^2)\exp(i\alpha x^2 + i\mu_c), \quad (9)$$

$$\psi_3(x,t,\tau) = A\exp(-C_1x^2 + C_2x + C_3) \times \exp(i\alpha x^2 + i\gamma x - i\theta_c + i\mu_c), \quad (10)$$

and

$$\psi_{nc}(x,t,\tau) = A_{nc}\exp(-C_{1nc}x^2 + C_{2nc}x + C_{3nc}) \times \exp(i\alpha_{nc}x^2 + i\gamma_{nc}x - i\theta_{nc} + i\mu_{nc}), \quad (11)$$

where the nontrivial Gouy phase μ_{nc} is given by

$$\mu_{nc}(t,\tau) = \frac{1}{2}\arctan\left(\frac{z_I}{z_R}\right). \quad (12)$$

All the coefficients present in Eqs. (8)–(12) are written out in Appendixes A and B for the sake of clarity. The indices R and I stand for the real and imaginary parts of the complex numbers that appear in the solutions. As discussed in [11], $\mu_{nc}(t,\tau)$ and $\theta_{nc}(t,\tau)$ are phases that do not depend on the transverse position x. Different from the Gouy phase, $\theta_{nc}(t,\tau)$ is one phase that appears as we displace the slit from a given distance from the origin, which is dependent on the parameter d.

The intensity at the screen including the nonclassical path reads

$$I_{nc} = |\psi_1+\psi_2+\psi_3+\psi_{nc}|^2 = I_c + |\psi_{nc}|^2 + 2|\psi_1||\psi_{nc}|\cos\phi_{1nc} + 2|\psi_2||\psi_{nc}|\cos\phi_{2nc} + 2|\psi_3||\psi_{nc}|\cos\phi_{3nc}, \quad (13)$$

where

$$\phi_{1nc} = (\alpha-\alpha_{nc})x^2 - (\gamma+\gamma_{nc})x - (\theta_c-\theta_{nc}) + (\mu_c-\mu_{nc}), \quad (14)$$

$$\phi_{2nc} = (\alpha-\alpha_{nc})x^2 - \gamma_{nc}x + \theta_{nc} + (\mu_c-\mu_{nc}), \quad (15)$$

and

$$\phi_{3nc} = (\alpha-\alpha_{nc})x^2 + (\gamma-\gamma_{nc})x - (\theta_c-\theta_{nc}) + (\mu_c-\mu_{nc}) \quad (16)$$

are the relative phases of ψ_1 and ψ_{nc}, ψ_2 and ψ_{nc}, and ψ_3 and ψ_{nc}, respectively, which implies that the interference is a result of two paths, as observed in [34]. I_c is the intensity when only classical paths are taken into account.

To quantify the deviations in the intensity produced by the existence of nonclassical paths we use the Sorkin parameter as defined in Refs. [32,33], i.e.,

$$\kappa I_0 = I_{nc} - I_c = |\psi_{nc}|^2 + 2|\psi_1||\psi_{nc}|\cos\phi_{1nc} + 2|\psi_2||\psi_{nc}|\cos\phi_{2nc} + 2|\psi_3||\psi_{nc}|\cos\phi_{3nc}, \quad (17)$$

where I_0 is the intensity at the central maximum. As we can observe, the parameter κ used to estimate the existence of the nonclassical path in the triple-slit interference is dependent on the Gouy phase difference between classical and nonclassical paths.

III. SORKIN PARAMETER AND GOUY PHASE FOR ELECTRON WAVES

In this section we analyze the Gouy phase effect in the quantity κ for electron waves. First, we observe the behavior of the normalized intensity and the parameter κ as a function of x while fixing the values of t and τ. We observe a displacement in the behavior of κ as an effect of the Gouy phase, which makes clear the role of this phase in the exact estimation of κ. The selected path 123 of Fig. 1 produces an asymmetric aspect for κ. But as we observe next, the symmetric aspect is restored if path 321 is also included. Second, we observe the behavior of the parameter κ as a function of x and τ while fixing the value of t, from which we can observe an upper bound for a given value of x and τ. Third, we consider the position $x = 0$ and observe the behavior of the parameter κ as a function of τ for t fixed. For $x = 0$ the Gouy phase effect is most evident since some other phases disappear in the interference, as we can see in Eqs. (14)–(16). As a matter of fact we can study the effect of all phases that appear with the nonclassical path since we know the analytic expression for them, but we analyze here only the Gouy phase effect, which can be measured for matter waves. Moreover, it is possible to tune parameters t and τ, σ_0, β, and d in order to study a specific phase contribution.

To construct the graphic of the intensity and the Sorkin parameter κ we consider an electron wave of wavelength $\lambda \approx 50$ pm and adopt the following parameters: $m = 9.11 \times 10^{-31}$ kg, $d = 650$ nm, $\beta = 62$ nm, $\sigma_0 = 62$ nm, $t = 18$ ns, $\tau = 15$ ns. For this value of wavelength the propagation velocity in the z direction is $v_z \approx 1.46 \times 10^7$ m/s, which corresponds to propagation distances much larger than the wavelength, i.e., $z_t \approx 26.3$ cm and $z_\tau \approx 21.9$ cm, respectively, before and after the triple slit. Using these parameters as input, we find $\epsilon = 0.492$ ns. In Fig. 2(a) we show the normalized intensity I_n as a function of x, which shows the shape of the intensity at the far field or Fraunhofer theory, as similarly observed in [31,32]. In Fig. 2(b) we show the Sorkin parameter κ as a function of x in which we consider (solid line) and we do not consider (dotted line) the Gouy phase effect. In accordance with [32] we find that the quantity κ is of the order of 10^{-8}, which corroborates our simplified analysis. Moreover, we verify numerically that the factor $|\psi_{nc}(x,t,\tau)|^2$ does not change the parameter κ significantly, with the main contributions coming from the crossed terms which contain the Gouy phase.

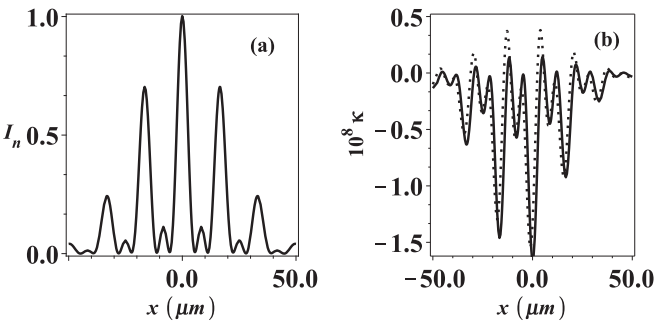

FIG. 2. (a) Normalized intensity as a function of x. (b) Sorkin parameter κ as a function of x. For the solid line we consider and for the dotted line we do not consider the Gouy phase difference.

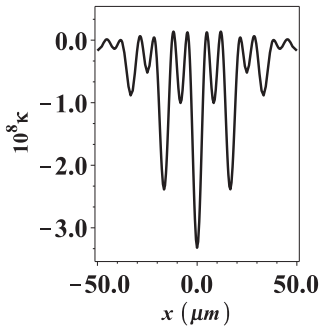

FIG. 3. Sorkin parameter κ as a function of x for two selected nonclassical paths, i.e., paths 123 and 321. As we can observe, κ is symmetric with respect to the change x by $-x$.

The asymmetric aspect of the factor κ shown in Fig. 2(b) is a consequence of the fact that we take only one nonclassical path, i.e., path 123 as presented in Fig. 1. If we also added nonclassical path 321, the symmetric aspect would be obtained, as we can observe in Fig. 3. Notice that the Sorkin parameter increases slightly with this additional contribution, as it should. Moreover, the parity symmetry is restored by adding such a complementary contribution.

In Fig. 4 we show the behavior of $|\kappa|$ as a function of x and τ for the nonclassical path shown in Fig. 1. We observe that it has a maximum for a given value of x and τ. The existence of a maximum enables us to choose a set of values of parameters that produce a value of κ which can be more accessible to being measured. The existence of a maximum value for this parameter as a function of the quantities involved in the experimental apparatus was previously observed in [33]. As we can see, this maximum occurs around $x = 0$. Next we will explore the Gouy phase effect to estimate the parameter κ for $x = 0$ since for this position some phases disappear, making the Gouy phase effect most evident.

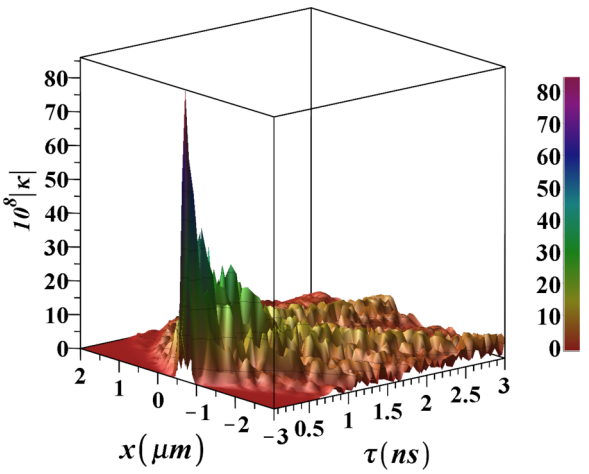

FIG. 4. Absolute value of Sorkin parameter κ as a function of τ and x for fixed t. It presents a maximum value for a given value of x and τ.

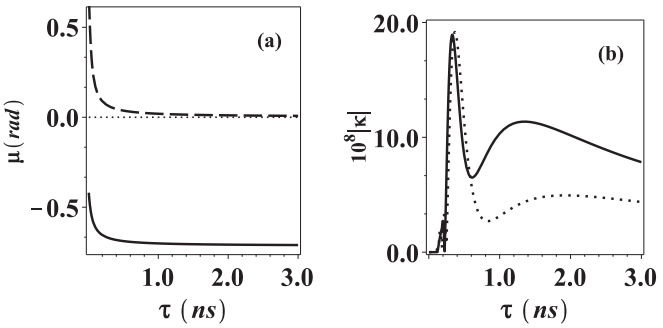

FIG. 5. (a) Gouy phase difference as a function of τ and fixed t. (b) Absolute value of the Sorkin parameter κ as a function of τ at $x = 0$ and fixed t. For solid line we consider and for dotted line we do not consider the Gouy phase difference.

In Fig. 5(a) we show the Gouy phase of the classical path (dashed line) and the nonclassical path in Fig. 1 (solid line) as a function of τ for the same parameters used above. We can observe that the absolute value of the Gouy phase for the classical path decreases, whereas for the nonclassical path it increases as the time propagation τ grows. This change affects the parameter κ. To observe such an effect, in Fig. 5(b) we show the absolute value of the parameter κ for the nonclassical path in Fig. 1 as a function of τ for $x = 0$. For the solid line we consider and for the dotted line we do not consider the Gouy phase difference.

The behavior of the parameter κ as a function of τ is similar to that obtained as a function of the distance of the triple slit to the screen in Ref. [33]. For a given value of τ it has a peak as in Ref. [33]. It is noteworthy that an exact solution for κ depends on the Gouy phase. In order to evaluate the effect of the Gouy phase on the absolute value of the parameter κ for the nonclassical path in Fig. 1, we calculate for point $x = 0$ the percentage error, which is defined by $(||\kappa| - |\kappa'||/|\kappa|) \times 100\%$, where for $|\kappa|$ we consider the Gouy phase difference which corresponds to the exact value and for $|\kappa'|$ we neglect the Gouy phase difference. Choosing $\tau = 2$ ns, the percentage error is 51.5%. Therefore if the Gouy phase is neglected, the parameter κ is misestimated. As we can observe in Fig. 5(a) for $\tau = 2$ ns, the Gouy phase of the classical path tends to zero, and the Gouy phase difference is due to the phase of the nonclassical path contribution, i.e., $\mu_c - \mu_{nc} \approx |\mu_{nc}| \approx 0.719$ rad. If one uses these parameters, one measures the Gouy phase difference as a signature of the nonclassical path contributions.

We observe that the effect of nonclassical paths in multislit matter-wave interferometry can be assessed by measuring the quantity κ as well as the Gouy phase corresponding to the wave function for this exotic trajectory, i.e., μ_{nc}. That is because, for a certain class of parameters, the Gouy phase difference is exactly (or approximately) the Gouy phase of the nonclassical path. Therefore the measurement of the Gouy phase difference amounts to the Gouy phase of nonclassical paths only from which the κ parameter may be inferred. On the other hand, in order to measure the Gouy phase using a multislit apparatus, a useful approach is proposed in Ref. [11], in which the Gouy phase is estimated by measuring the relative intensity and the fringe visibility, which are accessible quantities independent of the size of κ.

IV. CONCLUDING REMARKS

We studied the effects of a selected nonclassical path in the interference pattern in a triple-slit experiment. We solved exactly a one-dimensional model of propagation through a triple slit and found analytical expressions for the wave functions of classical and nonclassical paths. We obtained an exactly solution for the Sorkin parameter κ used to estimate the effect of the nonclassical path. The value of κ for electron waves is consistent with other results previously obtained for it, which makes our model reasonably good for studying the existence of the nonclassical path. We used the uncertainty in momentum to estimate the interslit propagation linking the existence of the nonclassical path with the uncertainty principle which is intuitive because of Feynman's path-integral formalism. The Gouy phases of classical and nonclassical paths are different, which contributes significantly to the value of κ. We observed the changing behavior of κ as a consequence of the Gouy phase difference for electron waves. We estimated the percentage error in the absolute value of parameter κ as a consequence of the Gouy phase difference for $x = 0$, $t = 18$ ns, and $\tau = 2$ ns and found 51.5%. We conclude, from the enormous discrepancy found, that the Gouy phase difference cannot be neglected in the three-slit interference if nonclassical paths are present. We expect that our results which connect the Sorkin parameter and Gouy phase will be useful for detecting the nonclassical path's effect by measuring the Gouy phase.

ACKNOWLEDGMENTS

The authors would like to thank CNPq Brazil for financial support. I.G.d.P. is thankful for support from the program PROPESQ (UFPI/PI) under Grant No. PROPESQ 23111.011083/2012-27.

APPENDIX A: FORMULAS FOR INTERFERENCE PARAMETERS

In the following we display the complete expressions for terms in Eqs. (8), (2), (10), and (11):

$$A = \frac{m}{2\hbar\sqrt{\sqrt{\pi}t\tau\sigma_0}}\left[\left(\frac{m^2}{4\hbar^2 t\tau} - \frac{1}{4\beta^2\sigma_0^2}\right)^2 + \frac{m^2}{16\hbar^2}\left(\frac{1}{\beta^2 t} + \frac{1}{\sigma_0^2 t} + \frac{1}{\sigma_0^2\tau}\right)^2\right]^{-\frac{1}{4}}, \tag{A1}$$

$$C_1 = \frac{\frac{m^2}{\hbar^2\tau^2}\mathcal{A}}{4[\mathcal{A}^2 + \mathcal{B}^2]}, \tag{A2}$$

$$C_2 = \frac{\frac{2md}{\hbar\tau\beta^2}\mathcal{B}}{4[\mathcal{A}^2+\mathcal{B}^2]},$$

$$\mathcal{A} = \left(\frac{1}{2\beta^2} + \frac{m^2\sigma_0^2}{2(\hbar^2t^2+m^2\sigma_0^4)}\right),$$

$$\mathcal{B} = \left(\frac{m^3\sigma_0^4}{2\hbar t(\hbar^2t^2+m^2\sigma_0^4)} - \frac{m}{2\hbar t} - \frac{m}{2\hbar\tau}\right),$$

$$C_3 = -\frac{d^2}{2\beta^2} + \frac{\hbar^2\tau^2d^2}{m^2\beta^2}C_1, \quad \gamma = \frac{2d\hbar\tau}{m\beta^2}C_1, \tag{A3}$$

$$\alpha = \frac{m}{2\hbar\tau} + \frac{m\beta^2}{2\hbar\tau}C_2, \;\; \theta_C = \frac{\hbar\tau d}{2m\beta^2}C_2, \tag{A4}$$

$$\mu_c(t,\tau) = -\frac{1}{2}\arctan\left[\frac{t+\tau\left(1+\frac{\sigma_0^2}{\beta^2}\right)}{\tau_0\left(1-\frac{t\tau\sigma_0^2}{\tau_0^2\beta^2}\right)}\right], \tag{A5}$$

$$A_{nc} = \sqrt{\frac{m^3\sqrt{\pi}}{16\hbar^3\tau t\epsilon\sigma_0\sqrt{z_R^2+z_I^2}}}, \tag{A6}$$

$$C_{1nc} = \frac{m^2z_{3R}}{4\hbar^2\tau^2\left(z_{3R}^2+z_{3I}^2\right)}, \tag{A7}$$

$$C_{2nc} = \frac{m^3dz_{6I}}{32\hbar^3\beta^2\tau\epsilon^2\left(z_{6R}^2+z_{6I}^2\right)} + \frac{mdz_{3I}}{2\hbar\tau\beta^2\left(z_{3R}^2+z_{3I}^2\right)}, \tag{A8}$$

$$C_{3nc} = \frac{d^2z_{1R}}{4\beta^4\left(z_{1R}^2+z_{1I}^2\right)} - \frac{m^2d^2z_{4R}}{64\beta^4\hbar^2\epsilon^2\left(z_{4R}^2+z_{4I}^2\right)} + \frac{m^4d^2z_{5R}}{4^5\hbar^4\beta^4\epsilon^4\left(z_{5R}^2+z_{5I}^2\right)} + \frac{m^2d^2z_{6R}}{32\beta^4\epsilon^2\hbar^2\left(z_{6R}^2+z_{6I}^2\right)} + \frac{d^2z_{3R}}{4\beta^4(z_{3R}^2+z_{3I}^2)} - \frac{d^2}{\beta^2}, \tag{A9}$$

$$\alpha_{nc} = \frac{m}{2\hbar\tau} + \frac{m^2z_{3I}}{4\hbar^2\tau^2\left(z_{3R}^2+z_{3I}^2\right)}, \tag{A10}$$

$$\gamma_{nc} = \frac{m^3dz_{6R}}{32\hbar^3\beta^2\tau\epsilon^2\left(z_{6R}^2+z_{6I}^2\right)} + \frac{mdz_{3R}}{2\hbar\tau\beta^2\left(z_{3R}^2+z_{3I}^2\right)}, \tag{A11}$$

$$\theta_{nc} = \frac{d^2z_{1I}}{4\beta^4\left(z_{1R}^2+z_{1I}^2\right)} - \frac{m^2d^2z_{4I}}{64\beta^4\hbar^2\epsilon^2\left(z_{4R}^2+z_{4I}^2\right)} + \frac{m^4d^2z_{5I}}{4^5\hbar^4\beta^4\epsilon^4\left(z_{5R}^2+z_{5I}^2\right)} + \frac{m^2d^2z_{6I}}{32\beta^4\epsilon^2\hbar^2\left(z_{6R}^2+z_{6I}^2\right)} + \frac{d^2z_{3I}}{4\beta^4\left(z_{3R}^2+z_{3I}^2\right)}, \tag{A12}$$

APPENDIX B: GOUY PHASE COMPONENTS

In the following we present the full expressions for the terms in Eq. (12).

$$z_R = (z_{0R}z_{1R} - z_{0I}z_{1I})(z_{2R}z_{3I} + z_{2I}z_{3R}) + (z_{0R}z_{1I} + z_{0I}z_{1R})(z_{2R}z_{3R} - z_{2I}z_{3I}), \tag{B1}$$

$$z_I = (z_{0R}z_{1R} - z_{0I}z_{1I})(z_{2R}z_{3R} - z_{2I}z_{3I}) - (z_{0R}z_{1I} + z_{0I}z_{1R})(z_{2R}z_{3I} + z_{2I}z_{3R}), \tag{B2}$$

$$z_{0R} = \frac{1}{2\sigma_0^2}, \quad z_{0I} = -\frac{m}{2\hbar t}, \tag{B3}$$

$$z_{1R} = \frac{1}{2\beta^2} + \frac{m^2z_{0R}}{4\hbar^2t^2\left(z_{0R}^2+z_{0I}^2\right)}, \tag{B4}$$

$$z_{1I} = -\left(\frac{m}{4\hbar\epsilon} + \frac{m}{2\hbar t} + \frac{m^2z_{0I}}{4\hbar^2t^2(z_{0R}^2+z_{0I}^2)}\right), \tag{B5}$$

$$z_{2R} = \frac{1}{2\beta^2} + \frac{m^2z_{1R}}{16\hbar^2\epsilon^2\left(z_{1R}^2+z_{1I}^2\right)}, \tag{B6}$$

$$z_{2I} = -\left(\frac{m}{2\hbar\epsilon} + \frac{m^2z_{1I}}{16\hbar^2\epsilon^2\left(z_{1R}^2+z_{1I}^2\right)}\right), \tag{B7}$$

$$z_{3R} = \frac{1}{2\beta^2} + \frac{m^2 z_{2R}}{16\hbar^2\epsilon^2\left(z_{2R}^2 + z_{2I}^2\right)}, \tag{B8}$$

$$z_{3I} = -\left(\frac{m}{2\hbar\tau} + \frac{m}{4\hbar\epsilon} + \frac{m^2 z_{2I}}{16\hbar^2\epsilon^2(z_{2R}^2 + z_{2I}^2)}\right), \tag{B9}$$

$$z_{4R} = z_{1R}^2 z_{2R} - z_{1I}^2 z_{2R} - 2z_{1R}z_{1I}z_{2I}, \tag{B10}$$

$$z_{4I} = z_{1R}^2 z_{2I} - z_{1I}^2 z_{2I} + 2z_{1R}z_{1I}z_{2R}, \tag{B11}$$

$$z_{5R} = z_{3R}\left(z_{1R}^2 z_{2R}^2 - z_{1R}^2 z_{2I}^2 - z_{1I}^2 z_{2R}^2 + z_{1I}^2 z_{2I}^2 - 4z_{1R}z_{1I}z_{2R}z_{2I}\right) - 2z_{3I}\left(z_{1R}^2 z_{2R}z_{2I} - z_{1I}^2 z_{2R}z_{2I} + z_{1R}z_{1I}z_{2R}^2 - z_{1R}z_{1I}z_{2I}^2\right), \tag{B12}$$

$$z_{5I} = z_{3I}\left(z_{1R}^2 z_{2R}^2 - z_{1R}^2 z_{2I}^2 - z_{1I}^2 z_{2R}^2 + z_{1I}^2 z_{2I}^2 - 4z_{1R}z_{1I}z_{2R}z_{2I}\right) + 2z_{3R}\left(z_{1R}^2 z_{2R}z_{2I} - z_{1I}^2 z_{2R}z_{2I} + z_{1R}z_{1I}z_{2R}^2 - z_{1R}z_{1I}z_{2I}^2\right), \tag{B13}$$

$$z_{6R} = z_{1R}z_{2R}z_{3R} - z_{1R}z_{2I}z_{3I} - z_{1I}z_{2R}z_{3I} - z_{1I}z_{2I}z_{3R}, \tag{B14}$$

and

$$z_{6I} = z_{1R}z_{2R}z_{3I} + z_{1R}z_{2I}z_{3R} + z_{1I}z_{2R}z_{3R} - z_{1I}z_{2I}z_{3I}. \tag{B15}$$

[1] L. G. Gouy, C. R. Acad. Sci. Paris **110**, 1251 (1890).
[2] L. G. Gouy, Ann. Chim. Phys., Ser. 6 **24**, 145 (1891).
[3] T. D. Visser and E. Wolf, Opt. Commun. **283**, 3371 (2010).
[4] R. Simon and N. Mukunda, Phys. Rev. Lett. **70**, 880 (1993).
[5] S. Feng and H. G. Winful, Opt. Lett. **26**, 485 (2001).
[6] J. Yang and H. G. Winful, Opt. Lett. **31**, 104 (2006).
[7] R. W. Boyd, J. Opt. Soc. Am. **70**, 877 (1980).
[8] P. Hariharan and P. A. Robinson, J. Mod. Opt. **43**, 219 (1996).
[9] S. Feng, H. G. Winful, and R. W. Hellwarth, Opt. Lett. **23**, 385 (1998).
[10] X. Pang, T. D. Visser, and E. Wolf, Opt. Commun. **284**, 5517 (2011); X. Pang, G. Gbur, and T. D. Visser, Opt. Lett. **36**, 2492 (2011); X. Pang, D. G. Fischer, and T. D. Visser, J. Opt. Soc. Am. A **29**, 989 (2012); X. Pang and T. D. Visser, Opt. Express **21**, 8331 (2013); X. Pang, D. G. Fischer, and T. D. Visser, Opt. Lett. **39**, 88 (2014).
[11] C. J. S. Ferreira, L. S. Marinho, T. B. Brasil, L. A. Cabral, J. G. G. de Oliveira, Jr., M. D. R. Sampaio, and I. G. da Paz, Ann. Phys. (NY) **362**, 473 (2015).
[12] D. Chauvat, O. Emile, M. Brunel, and A. Le Floch, Am. J. Phys. **71**, 1196 (2003).
[13] N. C. R. Holme, B. C. Daly, M. T. Myaing, and T. B. Norris, Appl. Phys. Lett. **83**, 392 (2003).
[14] W. Zhu, A. Agrawal, and A. Nahata, Opt. Express **15**, 9995 (2007).
[15] T. Feurer, N. S. Stoyanov, D. W. Ward, and K. A. Nelson, Phys. Rev. Lett. **88**, 257402 (2002).
[16] A. Hansen, J. T. Schultz, and N. P. Bigelow, in *Conference on Coherence and Quantum Optics, M6 66* (Optical Society of America, Rochester, New York, 2013); J. T. Schultz, A. Hansen, and N. P. Bigelow, Opt. Lett. **39**, 4271 (2014).
[17] G. Guzzinati, P. Schattschneider, K. Y. Bliokh, F. Nori, and J. Verbeeck, Phys. Rev. Lett. **110**, 093601 (2013); P. Schattschneider, T. Schachinger, M. Stöger-Pollach, S. Löffler, A. Steiger-Thirsfeld, K. Y. Bliokh, and F. Nori, Nat. Commun. **5**, 4586 (2014).
[18] T. C. Petersen, D. M. Paganin, M. Weyland, T. P. Simula, S. A. Eastwood, and M. J. Morgan, Phys. Rev. A **88**, 043803 (2013).
[19] A. E. Siegman, *Lasers* (University Science Books, Sausalito, CA, 1986).
[20] Ph. Balcou and A. L'Huillier, Phys. Rev. A **47**, 1447 (1993); M. Lewenstein, P. Salieres, and A. L'Huillier, *ibid.* **52**, 4747 (1995); F. Lindner, W. Stremme, M. G. Schatzel, F. Grasbon, G. G. Paulus, H. Walther, R. Hartmann, and L. Struder, *ibid.* **68**, 013814 (2003).
[21] F. Lindner, G. G. Paulus, H. Walther, A. Baltuška, E. Goulielmakis, M. Lezius, and F. Krausz, Phys. Rev. Lett. **92**, 113001 (2004).
[22] L. Allen, M. W. Beijersbergen, R. J. C. Spreeuw, and J. P. Woerdman, Phys. Rev. A **45**, 8185 (1992); L. Allen, M. Padgett, and M. Babiker, Prog. Opt. **39**, 291 (1999).
[23] S. Sato and S. Kawamura, J. Phys. Conf. Ser. **122**, 012025 (2008).
[24] I. G. da Paz, M. C. Nemes, S. Padua, C. H. Monken, and J. G. Peixoto de Faria, Phys. Lett. A **374**, 1660 (2010).
[25] I. G. da Paz, P. L. Saldanha, M. C. Nemes, and J. J. Peixoto de Faria, New J. Phys. **13**, 125005 (2011).
[26] R. Ducharme and I. G. da Paz, Phys. Rev. A **92**, 023853 (2015).
[27] H. Yabuki, Int. J. Theor. Phys. **25**, 159 (1986).
[28] R. P. Feynman and A. R. Hibbs, *Quantum Mechanics and Path Integrals*, 3rd. ed. (McGraw-Hill, New York, 1965).
[29] R. D. Sorkin, Mod. Phys. Lett. A **09**, 3119 (1994).
[30] U. Sinha, C. Couteau, T. Jennewein, R. Laflamme, and G. Weihs, Science **329**, 418 (2010).
[31] H. De Raedt, K. Michielsen, and K. Hess, Phys. Rev. A **85**, 012101 (2012).
[32] R. Sawant, J. Samuel, A. Sinha, S. Sinha, and U. Sinha, Phys. Rev. Lett. **113**, 120406 (2014).
[33] A. Sinha, A. H. Vijay, and U. Sinha, Sci. Rep. **5**, 10304 (2015).
[34] D. K. Park, O. Moussa, and R. Laflamme, New J. Phys. **14**, 113025 (2012).

[35] I. Söllner, Found. Phys. **42**, 742 (2012); G. Niestegge, *ibid.* **43**, 805 (2013); M. N. Bera, T. Qureshi, M. A. Siddiqui, and A. K. Pati, Phys. Rev. A **92**, 012118 (2015).
[36] J. S. M. Neto, L. A. Cabral, and I. G. da Paz, Eur. J. Phys. **36**, 035002 (2015).
[37] A. Zeilinger, R. Gähler, C. G. Shell, and W. Treimer, Rev. Mod. Phys. **60**, 1067 (1988).
[38] P. R. Berman, *Atom Interferometry* (Academic, San Diego, 1997), p. 175.
[39] A. Viale, M. Vicari, and N. Zanghi, Phys. Rev. A **68**, 063610 (2003).
[40] M. Beau and T. C. Dorlas, Int. J. Theor. Phys. **54**, 1882 (2015).
[41] O. C. O. Dahlsten, A. J. P. Garner, and V. Vedral, Nat. Commun. **5**, 4592 (2014).